ELSEVIER

Journal of Photochemistry and Photobiology A: Chemistry 154 (2003) 169–177

Journal of Photochemistry and Photobiology A:Chemistry

www.elsevier.com/locate/jphotochem

A novel family of twisted molecular luminescent materials containing carbazole unit for single-layer organic electroluminescent devices

Weihong Zhu, Meng Hu, Rong Yao, He Tian*

Institute of Fine Chemicals, East China University of Science & Technology, Shanghai 200237, PR China

Received 4 May 2002; received in revised form 14 July 2002; accepted 29 August 2002

Abstract

A novel family of twisted naphthalimide–carbazole dyads (NI–VK) and triads (NI–VK–NI) with moieties capable of carrier-balance and electroluminescence was synthesized. The key molecular structure design includes the use of carrier-transporting fragments, together with aliphatic side groups that can eliminate the recrystallization tendency and favor the formation of stable amorphous state. It shows that there exists an effective singlet–singlet energy transfer in dyads (NI–VK) and triads (NI–VK–NI) due to the overlap between the absorption of naphthalimide moiety and the emission of carbazole moiety. Such promising twisted emitters with glass-transition temperature of $T_g > 115\,^\circ\mathrm{C}$, which can generate stable cation and anion radicals for exciton recombination, were successfully utilized in single-layer electroluminescent (EL) device to avoid the layer–layer exciton quenching and micro-cavity effect. The single- and multi-layer devices fabricated with these compounds have been studied in an effort to improve the device efficiency and to gain insight into the luminescent mechanism. As for typical preliminary single-layer EL devices, only emission from naphthalimide was observed with maximum luminescence of 260 cd/m^2 at the driving voltage of 18 V.

Keywords: Single-layer OLED; Carbazole; Naphthalimide; Luminescence

---

1. Introduction

Organic electroluminescent (EL) devices are of great interest because of their efficient emission in the visible region and their potential application in full color large-area flat panel displays [1]. Electroluminescence in polymeric or molecular materials is obtained by the recombination of electrons and holes injected at the anode and the cathode, respectively. Much effort has been put into the development of new organic EL molecular materials and appropriate device structures to get high-efficiency and stable devices with defined emission colors [2–6]. One reason is that low molecular weight materials can be fabricated into homogenous films with fewer defects by using high-vacuum deposition technology. The easy purification and high quantum efficiency of small molecules is another reason for the success of the EL devices [7].

To achieve high luminescent efficiency, a multi-layer structure with hole and electron-transporting layers was usually employed to facilitate charge injection and transport. Such structure allows for inserting hole- or electron-blocking layers adjacent to the emission layer to maximize recombination of carriers. However, the fabrication of multi-layer devices is tedious and difficult to select the appropriate to optimize the device performance. To solve this problem, the blend polymers [8,9] or dopants [10] as emitters sandwiched between two electrodes (typical single-layer sandwiched EL device) is a good choice. However, the complication of doping, such as low morphological stability, phase-separation and low well-distribution, dramatically reduces device operation life-time. Considering these disadvantages, it is an alternative way to synthesize bipolar emitters that possess both a hole-transporting segment and an electron affinitive segment in order to enhance the charge injection/transport ability. Recently, several groups have reported single-layer OLED [11–13]. Hanack and coworkers reported maximum luminance of single-layer OLED with 2.5 cd/m^2 at a driving voltage of 20 V [11]. Bock and coworkers also demonstrated a single-layer OLED with 100 cd/m^2 [12]. When this strategy is extended, it is possible to obtain three-in-one molecules possessing emitting, electron and hole-transporting characteristics for single-layer OLED [2].

Naphthalimide derivatives usually exhibit strong fluorescent emission on irradiation, which are well known to act

---

* Corresponding author. Fax: +86-21-64252288.
E-mail address: tianhe@ecust.edu.cn (H. Tian).

1010-6030/03/$ – see front matter © 2003 Elsevier Science B.V. All rights reserved.
PII: S1010-6030(02)00325-8

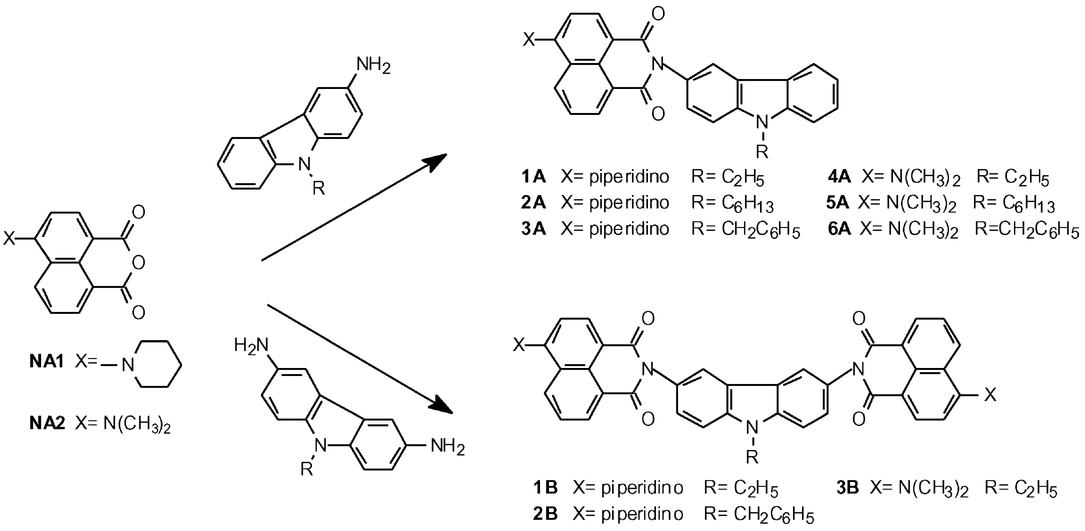

Scheme 1. Synthetic route of NI–VK and NI–VK–NI compounds.

as supermolecular moieties for the study of photo-induced electron transfer [14,15], fluorescence switcher [16] or liquid crystal displays [17]. Recently, a great light has been shed on naphthalimide utilized as EL materials [12,18–20]. The fluorescence emission can be widely tuned (from blue to yellow, green and even red) with amino- and alkoxy-groups at the 4-position of naphthalimide. It implies that naphthalimide derivatives are a new type of electron-transporting emitting materials for full color with high performance, such as good photo-stability, high fluorescent quantum yield and high electron affinity (about 3.1 eV) [18]. In continuation of our previous interests in materials suitable for OLEDs [21–23], we further report the synthesis and photo-/electro-luminescent properties of the twisted carbazole–naphthalimide dyads (NI–VK) and novel triads (NI–VK–NI) shown in Scheme 1. As expected, the incorporation of hole-transporting carbazole moiety (HOMO level is 5.80 eV) could regulate the current flow and hence increase the internal quantum efficiency by improving charge carriers' balance. Compared to multi-layer EL device, such dyads and triads containing carrier-transporting moiety could be utilized in single-layer EL device to avoid the layer–layer exciton quenching and micro-cavity effects. Additionally, the characteristics of multi-layer devices fabricated with these compounds have also been studied in an effort to improve the device efficiency and to gain insight into the luminescent mechanism.

2. Experimental

UV-Vis spectra were recorded on a Shimdatzu UV-260 spectrometer and fluorescence spectra were determined with a Hitachi-850 fluorescence spectrometer. ^{1}H NMR spectra were recorded on a Brucker AM500 spectrometer with tetramethylsilane as internal reference. Mass spectra were obtained on a Hitachi M80 instruments or Mariner time-of-flight (TOF, TIS ion source, PE Corp.). Infrared spectra were measured on a Shimidzu IR-408. Elemental analysis data were obtained on a Perkin-Elmer 240c instrument. Glass-transition temperatures (T_g) were measured using a differential scanning calorimeter TA DSC 2910 Instrument at a scan rate of 10 °C/min. All solvents were distilled prior to use. Reactions were monitored by thin-layer chromatography.

2.1. General procedure for synthesizing carbazole–naphthalimide dyads and triads

The synthetic route was illustrated in Scheme 1. Amino-substituted *N*-alkylcarbazole was prepared according to the literature [24]. A mixture of 4-substituted-1,8-naphthalic anhydride (NA1 or NA2), amino-substituted *N*-alkylcarbazole, piperidine (as catalyst) and 2-methoxyethanol was refluxed for 8 h under argon atmosphere monitored by the thin layer chromatography (TLC). After standing overnight, the precipitate was filtered and recrystallized from absolute ethanol twice or three times to give pure target compounds, which were characterized by ^{1}H NMR, IR, MS and elemental analysis.

*2.1.1. Compound **1A** (6-piperidino-2-(9-ethyl-9H-carbazol-3-yl)-benzo[de]isoquinoline-1,3-dione)*

Yield 53%, mp >270 °C. IR (KBr): 3030, 2930, 2910, 1700, 1650, 1585, 1490, 1450, 1360, 1340, 1230, 800, 780, 760, and 730 cm^{-1}. ^{1}H NMR (in d$_6$-DMSO): 1.36 (t, $J = 7.0$ Hz, 3H, –NCH$_2$**CH$_3$**), 1.64 (t, 2H, piperidine ring), 1.84 (m, 4H, piperidine ring), 3.23 (m, 4H, piperidine ring), 4.50 (q, 2H, –N**CH$_2$**CH$_3$), 7.20 (t, $J = 7.4$, and 7.5 Hz, 1H), 7.36 (d, $J = 8.2$ Hz, 1H), 7.39 (dd, $J = 8.5$, and 1.7 Hz, 1H), 7.48 (t, $J = 7.3$, and 8.2 Hz, 1H), 7.66 (d, $J = 8.2$ Hz, 1H), 7.70 (d, $J = 8.5$ Hz, 1H), 7.85 (t, $J = 8.2$, and 8.5 Hz, 1H), 8.10 (d, $J = 2.0$ Hz, 1H), 8.12 (d, $J = 7.1$ Hz, 1H), 8.42 (d, $J = 7.9$ Hz, 1H), 8.47 (d, $J = 8.2$ Hz, 1H), 8.50 (d, $J = 8.3$ Hz, 1H). MS (EI 70 eV), *m/e*: 474 (13.399%) [$M^+ + 1$], 473 (32.088%) [M^+]. Anal. calcd. for $\mathrm{C_{31}H_{27}N_3O_2}$: C 78.62%, H 5.75%, N 8.87%. Found: C 78.43%, H 5.53%, N 8.94%.

2.1.2. *Compound **2A** (6-piperidino-2-(9-hexyl-9H-carbazol-3-yl)-benzo[de]isoquinoline-1,3-dione)*

Yield 48%, mp 244–246 °C. IR (KBr): 3030, 2930, 2900, 1700, 1650, 1585, 1490, 1450, 1360, 1340, 1230, 800, 780, 750, and 730 $\mathrm{cm^{-1}}$. ^{1}H NMR (in $\mathrm{CDCl_3}$): 0.89 (t, $J = 7.0$ Hz, 3H, $\mathrm{CH_3}$–), 1.35 (m, 6H, –$\mathrm{(CH_2)_3}$–), 1.75 (t, 2H, piperidine ring), 1.92 (m, 6H, $-\mathrm{NCH_2}\mathbf{CH}_2-$ and piperidine ring), 3.28 (m, 4H, piperidine ring), 4.33 (t, $J = 7.2$ Hz, 2H, $-\mathrm{N}\mathbf{CH}_2\mathrm{CH_2}-$), 7.21 (t, $J = 7.6$, and 5.9 Hz, 1H), 7.24 (d, 1H), 7.37 (dd, $J = 8.5$, and 2.0 Hz, 1H), 7.42 (d, 1H), 7.46 (t, 1H), 7.52 (d, $J = 8.6$ Hz, 1H), 7.72 (d, $J = 7.40$ Hz, 1H), 8.03 (m, 2H), 8.46 (d, $J = 8.4$ Hz, 1H), 8.59 (d, $J = 8.0$ Hz, 1H), 8.65 (d, $J = 7.2$ Hz, 1H). MS (EI 70 eV), *m/e*: 529 (47.733%) [M^+]. Anal. calcd. for $\mathrm{C_{35}H_{35}N_3O_2}$: C 79.37%, H 6.66%, N 7.93%. Found: C 79.21%, H 6.57%, N 8.02%.

2.1.3. *Compound **3A** (6-piperidino-2-(9-benzyl-9H-carbazol-3-yl)-benzo[de]isoquinoline-1,3-dione)*

Yield 47%, mp > 270 °C. IR (KBr): 3030, 2960, 2630, 2900, 1700, 1650, 1580, 1490, 1460, 6 1380, 1350, 1220, 800, 780, and 720 $\mathrm{cm^{-1}}$. ^{1}H NMR (in $\mathrm{CDCl_3}$): 1.75 (t, $J = 6.0$ Hz, 2H, piperidine ring), 1.92 (m, 4H, piperidine ring), 3.28 (t, 4H, piperidine ring), 5.56 (s, 2H, $-\mathrm{N}\mathbf{CH}_2\mathrm{Ph}$), 7.26 (m, 7H), 7.33 (dd, $J = 8.5$, and 2.0 Hz, 1H), 7.42 (m, 2H), 7.50 (d, $J = 8.5$ Hz, 1H), 7.72 (q, $J = 8.4$, and 8.4 Hz, 1H), 8.01 (d, $J = 8.1$ Hz, 1H), 8.06 (d, $J = 1.9$ Hz, 1H), 8.46 (dd, $J = 8.5$, and 1.1 Hz, 1H), 8.57 (d, $J = 8.0$ Hz, 1H), 8.64 (dd, $J = 7.2$, and 1.1 Hz, 1H). MS (EI 70 eV), *m/e*: 536 (8.693%) [$M^+ + 1$], 535 (19.2%) [M^+]. Anal. calcd. for $\mathrm{C_{36}H_{29}N_3O_2}$: C 80.72%, H 5.46%, N 7.84%. Found: C 80.68%, H 5.49%, N 7.89%.

2.1.4. *Compound **4A** (6-dimethylamino-2-(9-ethyl-9H-carbazol-3-yl)-benzo[de]isoquinoline-1,3-dione)*

Yield 42%, mp >270 °C. IR (KBr): 3030, 2980, 2960, 2900, 1690, 1650, 1580, 1490, 1360, 1240, 1180, 1140, 780, and 740 $\mathrm{cm^{-1}}$. ^{1}H NMR (in $\mathrm{CDCl_3}$): 1.48 (t, $J = 7.2$ Hz, 3H, $\mathbf{CH}_3\mathrm{CH_2N}-$), 3.15 (s, 6H, $-\mathrm{N(CH_3)_2}$), 4.42 (q, $J = 7.2$ Hz, 2H, $\mathrm{CH_3}\mathbf{CH}_2\mathrm{N}-$), 7.17 (d, $J = 8.2$ Hz, 1H), 7.22 (d, $J = 8.3$, 7.4, and 1.0 Hz, 1H), 7.38 (d, $J = 8.5$, and 2.0 Hz, 1H), 7.41 (d, $J = 8.2$ Hz, 1H), 7.48 (d, $J = 8.2$, 7.0, and 1.0 Hz, 1H), 7.56 (d, $J = 8.5$ Hz, 1H), 7.72 (q, $J = 8.5$ Hz, $J = 8.5$ Hz, 1H), 8.03 (d, $J = 8.1$ Hz, 1H), 8.05 (s, 1H), 8.51 (dd, $J = 8.5$, and 1.1 Hz, 1H), 8.56 (d, $J = 8.2$ Hz, 1H), 8.65 (dd, $J = 7.2$, and 1.1 Hz, 1H). MS (EI 70 ev), *m/e*: 434 (21.934%) [$M^+ + 1$], 433 (55.976%) [M^+]. Anal. calcd. for $\mathrm{C_{28}H_{23}N_3O_2}$: C 77.58%, H 5.35%, N 9.69%. Found: C 77.63%, H 5.44%, N 9.58%.

2.1.5. *Compound **5A** (6-dimethylamino-2-(9-hexyl-9H-carbazol-3-yl)-benzo[de]isoquinoline-1,3-dione)*

Yield 51%, mp 240–242 °C. IR (KBr): 3030, 2960, 2930, 2900, 1695, 1650, 1580, 1490, 1460, 1360, 780, 750, and 730 $\mathrm{cm^{-1}}$. ^{1}H NMR (in $\mathrm{CDCl_3}$): 0.84 (t, $J = 7.0$ Hz, 3H, $-\mathrm{CH_2}\mathbf{CH}_3$), 1.34 (m, 6H, –$\mathrm{(CH_2)_3}$–), 1.91 (m, 2H, $-\mathrm{NCH_2}\mathbf{CH}_2\mathrm{CH_2}-$), 3.15 (s, 6H, $-\mathrm{N(CH_3)_2}$), 4.33 (t, $J = 7.2$ Hz, 2H, $-\mathrm{N}\mathbf{CH}_2\mathrm{CH_2}-$), 7.16 (d, $J = 8.2$ Hz, 1H), 7.21 (t, $J = 7.3$, and 7.4 Hz, 1H), 7.37 (dd, $J = 8.5$, and 1.0 Hz, 1H), 7.42 (d, $J = 8.2$ Hz, 1H), 7.47 (t, $J = 7.7$, and 7.3 Hz, 1H), 7.54 (d, $J = 8.5$ Hz, 1H), 7.71 (t, $J = 7.8$, and 7.9 Hz, 1H), 8.02 (d, $J = 8.0$ Hz, 1H), 8.04 (d, $J = 1.7$ Hz, 1H), 8.50 (d, $J = 8.4$ Hz, 1H), 8.55 (d, $J = 8.2$ Hz, 1H), 8.65 (d, $J = 7.1$ Hz, 1H). MS (EI 70 eV), *m/e*: 490 (100%) [$M^+ + 1$]. Anal. calcd. for $\mathrm{C_{32}H_{31}N_3O_2}$: C 78.50%, H 6.38%, N 8.58%. Found: C 78.59%, H 6.40%, N 8.64%.

2.1.6. *Compound **6A** (6-dimethylamino-2-(9-benzyl-9H-carbazol-3-yl)-benzo[de]isoquinoline-1,3-dione)*

Yield 55%, mp >270 °C. IR (KBr): 3030, 2960, 2940, 2900, 1695, 1650, 1580, 1490, 1460, 1360, 780, 750, and 730 $\mathrm{cm^{-1}}$. ^{1}H NMR (in $\mathrm{d_6}$-DMSO): 3.14(s, 6H, $-\mathrm{N(CH_3)_2}$), 5.75 (s, 2H, $-\mathbf{CH}_2\mathrm{Ar}$), 7.27 (m, 7H), 7.37 (dd, $J = 8.6$, and 2.0 Hz, 1H), 7.49 (d, $J = 7.3$, and 1.1 Hz, 1H), 7.72 (d, $J = 8.41$ Hz, 1H), 7.75 (d, $J = 8.7$ Hz, 1H), 7.81 (q, $J = 8.5$, and 8.5 Hz, 1H), 8.15 (d, $J = 2.0$ Hz, 1H), 8.17 (d, $J = 7.9$ Hz, 1H), 8.39 (d, $J = 8.3$ Hz, 1H), 8.50 (dd, $J = 7.2$, and 1.0 Hz, 1H), 8.79 (dd, $J = 8.5$, and 1.0 Hz, 1H). MS (EI 70 eV), *m/e*: 494 (69.857%) [$M^+ - 1$]. Anal. calcd. for $\mathrm{C_{33}H_{25}N_3O_2}$: C 79.98%, H 5.08%, N 8.48%. Found: C 79.92%, H 5.18%, N 8.49%.

2.1.7. *Compound **1B** (6-piperidino-2-[7-(6-piperidino-benzo[de]isoquinoline-1,3-dione-2-yl)-9-ethyl-9H-carbazol-3-yl]-benzo[de]isoquinoline-1,3-dione)*

Yield 52%, mp >270 °C. IR (KBr): 2930, 2860, 1700, 1670, 1585, 1490, 1460, 1360, 1230, 790, and 760 $\mathrm{cm^{-1}}$. ^{1}H NMR (in $\mathrm{d_6}$-DMSO) 1.45 (t, $J = 7.0$ Hz, 3H, $-\mathrm{NCH_2}\mathbf{CH}_3$), 1.68 (t, 4H, piperidine ring), 1.86 (m, 8H, piperidine ring), 3.23 (t, 8H, piperidine ring), 4.60 (q, $J = 7.0$ Hz, 2H, $-\mathrm{N}\mathbf{CH}_2\mathrm{CH_3}$), 7.36 (m, 2H), 7.45 (dd, $J = 8.7$, and 2.0 Hz, 2H), 7.79 (d, $J = 8.7$ Hz, 2H), 7.85 (m, 2H), 8.10 (d, $J = 2.0$ Hz, 2H), 8.43 (dd, $J = 8.0$, and 3.5 Hz, 2H), 8.80 (m, 4H). MALDI-TOF MS, *m/e*: 774.0067 [$M^+ + \mathrm{Na}$] (calcd. for $\mathrm{C_{48}H_{41}N_5O_4}^+ + \mathrm{Na}$ 774.3056). Anal. calcd. for $\mathrm{C_{48}H_{41}N_5O_4}$: C 76.68%, H 5.50%, N 9.31%. Found: C 76.62%, H 5.54%, N 9.37%.

2.1.8. *Compound **2B** (6-piperidino-2-[7-(6-piperidino-benzo[de]isoquinoline-1,3-dione-2-yl)-9-benzyl-9H-carbazol-3-yl]-benzo[de]isoquinoline-1,3-dione)*

Yield 62%, mp >270 °C. IR (KBr): 2930, 2860, 1700, 1670, 1590, 1490, 1460, 1360, 1235, 790, 760, and 730 $\mathrm{cm^{-1}}$. ^{1}H NMR (in $\mathrm{d_6}$-DMSO): 1.66 (t, 4H, piperidine ring), 1.83 (m, 8H, piperidine ring), 3.23 (t, 8H, piperidine ring), 5.80 (s, 2H, –N**CH**$_2$Ph), 7.29 (m, 2H), 7.34 (dd, 4H), 7.36 (s, 1H), 7.45 (dd, J = 9.0, and 1.9 Hz, 2H), 7.82 (m, 4H), 8.12 (d, J = 1.9 Hz, 2H), 8.40 (d, J = 8.2 Hz, 2H), 8.46 (dd, J = 7.3, 8.6 Hz, 4H). Anal. calcd. for $C_{53}H_{43}N_5O_4$: C 78.21%, H 5.32%, N 8.60%. Found: C 78.61%, H 5.37%, N 8.47%.

*2.1.9. Compound **3B** (6-dimethylamino-2-[7-(6-dimethyl-amino-benzo[de]isoquinoline-1,3-dione-2-yl)-9-ethyl-9H-carbazol-3-yl]-benzo[de]isoquinoline-1,3-dione)*

Yield 44%, mp >270 °C. IR (KBr): 2930, 2860, 1700, 1670, 1580, 1490, 1450, 1360, 1230, 780, and 760 cm^{-1}. ^{1}H NMR (in d$_6$-DMSO) 1.45 (t, J = 7.1 Hz, 3H, **CH**$_3$CH$_2$N–), 3.13 (s, 12H, –N(CH$_3$)$_2$), 4.60 (q, J = 7.1 Hz, 2H, CH$_3$**CH**$_2$N–), 7.27 (d, J = 8.4 Hz, 2H), 7.44 (dd, J = 8.6, and 2.0 Hz, 2H), 7.80 (m, 4H), 8.10 (d, J = 1.9 Hz, 2H), 8.38 (d, J = 8.3 Hz, 2H), 8.50 (dd, J = 7.3, and 1.0 Hz, 2H), 8.58 (d, J = 8.5 Hz, 2H). Anal. calcd. for $C_{42}H_{33}N_5O_4$: C 75.10%, H 4.95%, N 10.43%. Found: C 75.28%, H 5.12%, N 10.13%.

2.2. EL device fabrication and characterization

bis [2-(2-(Hydroxyphenyl)pyridinato]berylium (BePP$_2$), CuPc and TPD (N,N'-diphenyl-N,N'-bis(3-methylphenyl)-1,1′-diphenyl-4,4′-diamine) were used as received. When we made EL device using these compounds, all compounds have to be purified by means of vacuum sublimation, which was common method to get the optical characterizations of the new compounds. Typical single-layer EL devices 1 (ITO/compounds NI–VK or NI–VK–NI (50–100 nm)/LiF (1 nm)/AlLi) and multi-layer device 2 (ITO/CuPc (10 nm)/TPD (10 nm)/compound **4A** (30 nm)/BePP$_2$ (45 nm)/LiF (1 nm)/AlLi) were vacuum deposited at a pressure below 10^{-7} Torr. ITO-on-glass substrates (20 Ω/□) were cleaned ultrasonically and treated with oxygen plasma. The electrode area of the EL devices is 0.28 cm^2. The EL spectra were recorded on a PTI QM1 luminescence spectrometer. Device brightness was obtained from the measured photodiode currents, using the relationship between photocurrent and brightness measured on the PR-650. All measurements were carried out at room temperature under ambient atmosphere.

3. Results and discussion

The synthesis of carbazole–naphthalimide dyads is depicted in Scheme 1. 4-Bromo-1,8-naphthalic anhydride condensed readily with excess nucleophilc secondary amines (piperidine or dimethylamine) to give 4-piperidinonaphthalic anhydride (NA1) or 4-dimethylaminonaphthalic anhydride (NA2). Mono- or dinitro-N-alkylcarbazoles were prepared through two steps (phase-transferring catalytic alkylation and nitration) according to the literature [24]. The key intermediates mono- or diamino-N-alkylcarbazoles, which were prepared by the reduction of relative nitro-substituted N-alkylcarbazoles with stannous chloride in hydrochloric acid, could be used in the condensation without further purification. Because the basicity of the aromatic amine is much weaker than that of aliphatic amine, the imidization of NA1 or NA2 with relative amino-substituted N-alkylcarbazole undergoes with much more difficulty. However, the imidization of anhydride can be catalyzed by base or weak acid. We found the imidization could give satisfactory yield in 2-methoxyethanol with the base catalysis of piperidine. The molecular structures were confirmed by elemental analysis, infrared spectra, mass spectra and ^{1}H NMR.

The absorption and emission of the dyads and triads in chloroform are listed in Table 1. Comparing with 4-dimethylamino-N-ethyl-1,8-naphthalimide (its absorption peak at 415.6 nm in chloroform), the peak at about 409–415 nm is corresponding to the absorption of the naphthalimide moiety. Compared to N-dimethylamio analogues, a hypsochromic shift about 5 nm in N-piperidino derivatives is observed. All compounds display strong greenish-yellow fluorescence. Considering the emission of N-ethyl-4-dimethylamino-1,8-naphthalimide (λ^{ex}_{max} = 415.6 nm, λ^{fl}_{max} = 503 nm in CHCl$_3$), the fluorescence peak (500–512 nm) is originated from the naphthalimide moiety regardless of different excitation wavelengths, a case in point is the PL spectra of compound **6A** (curves b and c illustrated in Fig. 1). Although 3-amino-N-ethylcarbazole emitted light (peak at 355 nm in chloroform, curve d), the PL emission of carbazole moiety in NI–VK or NI–VK–NI was not detected. This shows that in such naphthalimide derivatives the emission of carbazole moiety is quenched,

Table 1
Absorption (λ^{ab}_{max}, nm) and fluorescence maximum wavelength (λ^{fl}_{max}, nm) of NI–VK and NI–VK–NI in CHCl$_3$ (2.5×10^{-5} mol/l)

	Compounds								
	1A	**2A**	**3A**	**4A**	**5A**	**6A**	**1B**	**2B**	**3B**
l^{ab}_{max}	267.4 (4.50)	268 (4.56)	265.6 (4.60)	267.6 (4.50)	268.0 (4.51)	264.8 (4.56)	269.8 (4.57)	267.6 (4.57)	268.8 (4.54)
$\log \varepsilon$	409.4 (4.07)	411.4 (4.14)	411.8 (4.15)	416.0 (4.07)	416.4 (4.07)	416.8 (4.13)	409.8 (4.27)	410.4 (4.32)	416.2 (4.26)
λ^{fl}_{max} [a]	510	511	511	503	507	500	510	509	504
ϕ_{fl} [b]		23.9	61.4	66.6	81.2	66.3	54.8	87.8	51.8

[a] The emissions were obtained by the excitation at relative longer absorption peak.

[b] The relative fluorescence quantum yields (ϕ_{fl}) of these compounds were measured by comparison with Rhodamine 6G as reference (defined as 1.00).

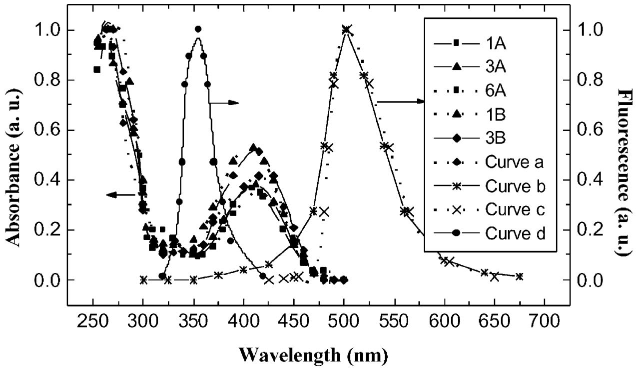

Fig. 1. Absorption spectra of carbazole–naphthalimide dyads **1A**, **3A**, **6A**, **1B**, and **3B** in $CHCl_3$. Curve a is the absorption of the equivalent-molar mixture of 3-amino-*N*-ethyl carbazole and 4-dimethylamino-*N*-ethyl-1,8-naphthalimide. Curves b and c are PL spectra of compound **6A** excited at 264.8 and 416.4 nm, respectively. Curve d is the PL spectra of 3-amino-*N*-ethylcarbazole excited at 265 nm.

which means that there exist an effective singlet–singlet energy transfer due to the overlap between the absorption of naphthalimide moiety and the emission of carbazole moiety.

Comparing with the absorption of the corresponding mixture of 1,8-naphthalimide and carbazole (shown in Fig. 1), the absorption of these novel dyads in solution is almost the sum of that of the constitute chromophores. It implies that there is no interaction between chromophores in their ground state. This is also explained according to the molecular conformation. As shown in Fig. 2, the optimized molecular structure of NI–VK calculated by using MOPAC AM1 and PM3 methods shows that the carbazole moiety is twisted by the steric hindrance of carbonyl group of naphthalimide, the dihedral angel between the plane of carbazole and naphthalimide units is 51.46°. Hence, the π-electron of carbazole moiety cannot delocalize to that of naphthalimide moiety and the individual absorption characteristics of the chromophores should be maintained. In addition, the N-substituted group of carbazole moiety is far away from the naphthalimide moiety and does not influence the absorption and fluorescence maximum wavelength of NI–VK dyads. Hence, such molecular assembly incorporating hole-transporting moiety into emitting unit does not change the degree of conjugation and the color of the original emitting chromophore. This could overcome the disadvantage that polymeric emitting light is dependent on the degree of conjugated polymers [20].

The photo-electronic equipment has to be designed to accept temperature excursions as high as 80 °C. To date, a number of stable organic glasses have been reported. A typical example is 4,4′,4″-tri(*N*-carbazolyl)triphenylamine (TCTA), a starburst molecule with a glass-transition temperature (T_g) as high as 151 °C described by Shirota and coworkers in 1994 [25]. Materials having high glass-transition temperatures are particularly desirable for enhancing the stability and lifetime of the devices [26,27]. In fact, such twisted non-planar molecular conformation and the alkyl substituted group of dyads (NI–VK) and triads (NI–VK–NI) can prevent easy spacial reorientation of the molecules, thus eliminating the recrystallization tendency and favoring the formation of stable amorphous state. The thermal stability of such compounds was determined on a differential scanning calorimeter (DSC) under the analysis program of 10 °C/min from 25 to 350 °C. As illustrated in Fig. 3, the initial heating trace of compound **4A** showed a sharp melting endothermic peak at 310 °C (the melting point, T_m). Then the sample was cooled down from the melt at the cooling rate of 10 °C/min, it spontaneously formed a supercooled liquid state. When the sample was heated again, an endothermic phenomenon was heated at 116 °C, at which the glassy state changed into the supercooled liquid state (T_g). Then a broad exothermic peak due to the crystallization was observed around 188 °C, followed by the endothermic peak due to the melting at 307 °C. Similar thermal properties with compound **2B** (T_g = 130.7 °C) was also observed in Fig. 4. However, no distinct glass-transition state was observed when compound **3A** was taken on the second heat (shown in Fig. 4). Thermal analysis results therefore, indicated that these dyads and triads

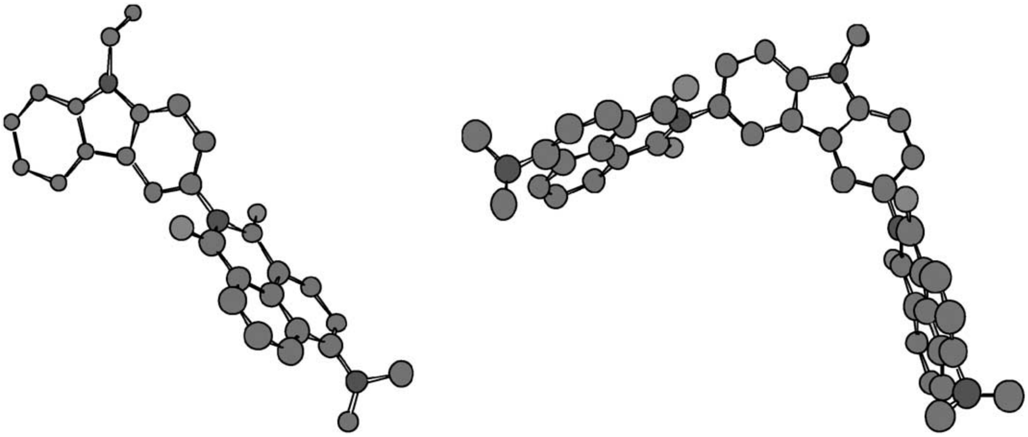

Fig. 2. Optimized molecular structure of compounds **4A** and **3B** calculated by using MOPAC AM1 and PM3 methods.

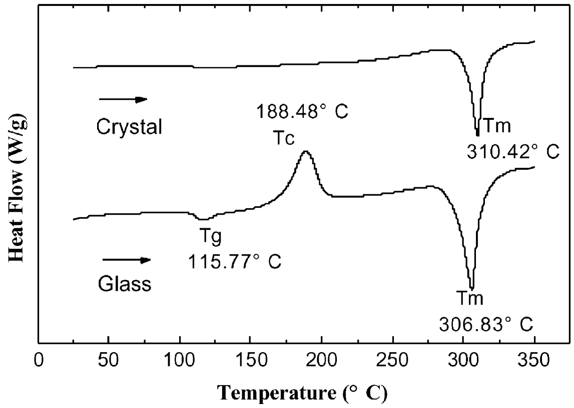

Fig. 3. Differential scanning calorimeter traces of compound **4A**.

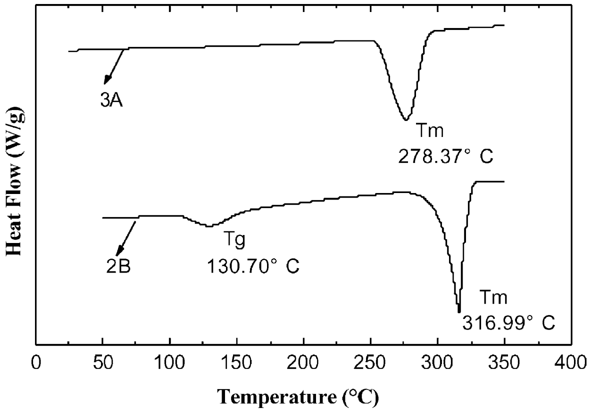

Fig. 4. Differential scanning calorimeter traces of compound **3A** and **2B**, taken on the second heat after cooled down from the melt at the cooling rate of 10 °C/min.

have relative high T_g and good thermal stability, which is very essential for fabricating stable organic EL devices.

Two types of EL devices were fabricated. Device 1 has an architecture of ITO/compounds NI–VK or NI–VK–NI (50–100 nm)/LiF (1 nm)/AlLi, which has only single-layer and only one molecular component between the electrodes. Device 2 has a architecture of ITO/CuPc (10 nm)/TPD (10 nm)/compound **4A** (30 nm)/BePP$_2$ (45 nm)/LiF (1 nm)/AlLi. To improve the performance of the two EL devices, a 1.0 nm LiF layer was inserted between the cathode and organic layer. Here, the thin layer acts as an insulating layer that allows sufficient potential differences to be maintained for better electron injection into emitter and prolong the lifetime of OLEDs [28].

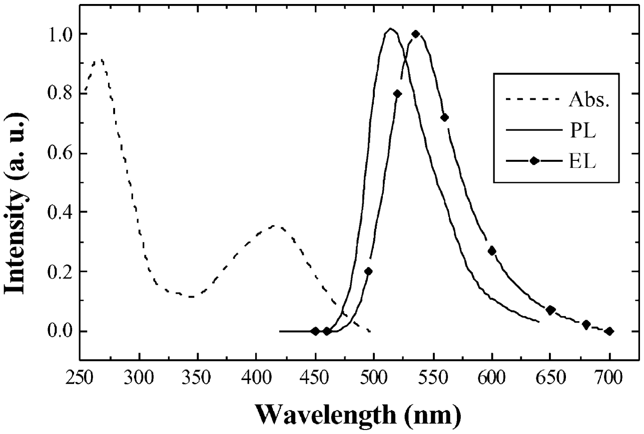

Fig. 5. Absorption, PL spectra of compound **4A** in CHCl$_3$ and EL spectrum (ITO/compound **4A** (53 nm)/LiF (1 nm)/AlLi).

As shown in Fig. 5, a case in point is only emission peak at 535 nm in single-layer device (ITO/compound **4A** (53 nm)/LiF (1 nm)/AlLi). Comparing with the PL spectrum of compound **4A** in chloroform, the EL spectrum peak was originated from the naphthalimide unit. There was a bathochromic shift of 20 nm compared to PL. The possible reason was that vibronic peak intensity was transferred to low energy in EL. Fig. 6 illustrated the typical luminescence–current density–voltage characteristics of the present single-layer device. The maximum brightness reached 110 cd/m^2 at a driving voltage of 21 V. Remarkably, the device has a maximum current density of 240 mA/cm^2.

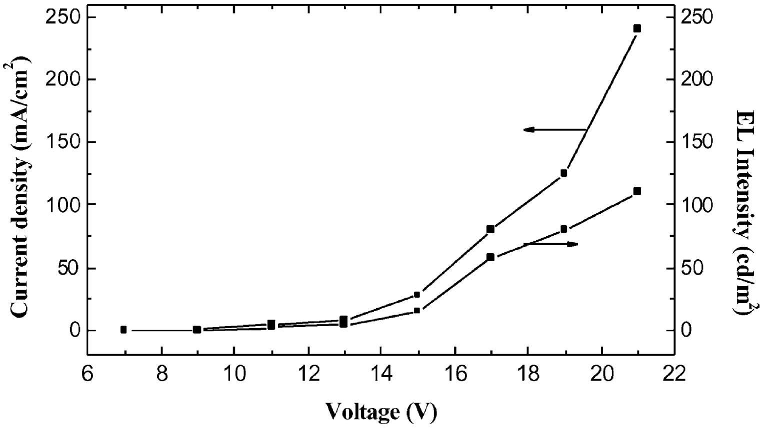

Fig. 6. Luminance–current density–voltage characteristics of EL device (ITO/compound **4A** (53 nm)/LiF (1 nm)/AlLi).

Table 2
EL data for the compounds NI–VK and NI–VK–NI

Compounds	Turn-on voltage (V)	λ_{EL} (nm)	Maximum brightness (cd/m^2)	Current density (mA/cm^2)
1A	12	539	87 (21)	202 (21)
2A	11	539	90 (20)	190 (20)
3A	11	540	120 (21)	260 (21)
4A	11	535	110 (21)	240 (21)
5A	Not determine			
6A	10	532	98 (18)	140 (18)
1B	7	539	238 (18)	271 (18)
2B	8	538	260 (18)	282 (18)
3B	8	534	224 (18)	253 (18)

Values given in parenthesis are expressed in volts.

Up to now, one had to take at least double or triple layer arrangements for an efficient OLED. It implies that such NI–VK dyads with introducing carrier-transporting unit could indeed increase the hole and electron injection and such molecular design maybe hopeful for exploring new functional molecules to fabricate single-layer EL device. In order to improve the performance of single-layer device, we also made the chemical structure modification and synthesized compound **1B**–**3B** (twisted triads NI–VK–NI). Table 2 outlined the preliminary single-layer devices characteristics (ITO/compounds NI–VK or NI–VK–NI (50–100 nm)/LiF (1 nm)/AlLi). In particular, triads (**1B**–**3B**) display higher brightness, lower turn-on voltage (defined as the voltage required to achieve a brightness of 1 cd/m^2) than that of dyads NI–VK, which suggest that incorporating two carbazole units in triads can increase carrier-transporting balance and prevent some percentage of electrons leaking up to the anode. As well known, the electron or hole thermodynamic transporting is dependent on orbital level. For our case, although the HOMO level (5.8 eV) is not so different from that of naphthalimide (5.5 eV), we believe the kinetics in the presence of carbazole unit play much role in the carrier mobility for the efficient EL generation, which can be characterized by the time-of-flight technique [29]. Actually, poly(vinycarbazole) (PVK) is a great promising hole-transporting and electron-blocking candidates. Moreover, such dyads and triads is a model for designing twisted oligomers, whose luminance is only dependent on the luminescent moiety.

We also studied the device 2 with introducing additional electron-transporting layer (BePP$_2$) and hole-transporting layer (CuPc and TPD), in an effort to improve the device

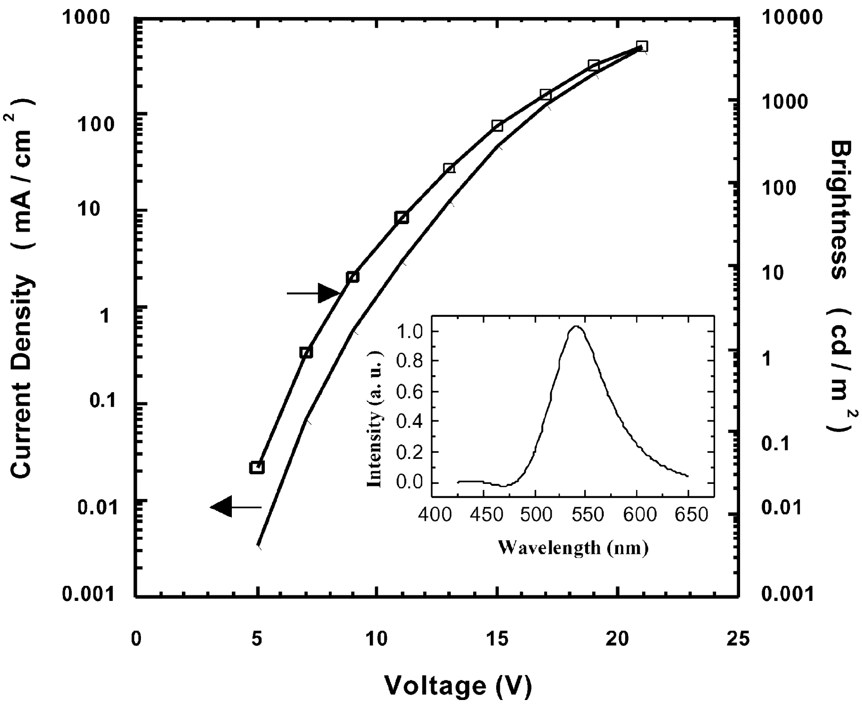

Fig. 7. EL spectrum and luminance–current density–voltage characteristics of device 2: ITO/CuPc (10 nm)/TPD (10 nm)/compound **4A** (30 nm)/BePP$_2$ (45 nm)/LiF (1 nm)/AlLi.

efficiency and to gain insight into the luminescent mechanism. Only emission from naphthalimide was also observed, i.e. identical to device 1. The maximum luminescence of the device 2 reached 4800 cd/m^2 at the driving voltage of 21 V, the maximum current density increased up to 410 mA/cm^2 (shown in Fig. 7). It is thought that the additional carrier-transporting layers increased carrier mobility and facilitated more carrier-injection.

In both EL devices 1 and 2, only greenish-yellow emission from naphthalimide moiety was observed and the carbazole unit did not emit light in the operation of the devices. This can be explained as follows, especially for the device 1 with the single-layer. Electrons are injected from cathode to the LUMO orbital of the high electron affinity naphthalimide moiety (about 3.1 eV) and holes are also injected from ITO (4.6 eV) to the HOMO orbital of carbazole moiety (HOMO level 5.8 eV). Then the holes are transferred intramolecularly to HOMO orbital of naphthalimide (ca. 5.5 eV). Hence, the holes and electrons recombine in the naphthalimide moiety to form excitons that undergo radiative decay resulting in the naphthalimide characteristic emission. The carbazole moiety indeed facilitates the hole injection and act as electron-blocking function.

In fact, it is anticipated that relatively stable cation radicals could be formed by blocking the 3, 6 and 9 positions of carbazole moiety in such NI–VK dyads in that the active ring sites are the two position *para* to the nitrogen atom [30]. The naphthalimide shows good thermal stability (because of the imide link) and high electron affinity EA (because of the carbonyl moiety), thus being favorable to obtain electron to form stable anion radicals [20]. Hence, such dyads possess the desired bipolar emitter character, generating stable cation and anion radicals for exciton recombination [31]. It implied that such design method, i.e. incorporating carrier-transporting unit into emitter unit via covalent bonds, is reasonable and effective. Further work to optimize EL devices of compounds NI–VK and NI–VK–NI is in progress.

4. Conclusions

We introduced a carbazole moiety as hole-transporting unit to develop a novel family of twisted luminescent naphthalimide derivatives for OLED applications. This led to the design and synthesis of novel yellow–green emitters with carrier-balance and sterically hindered structure. Such molecular assembly incorporating hole-transporting moiety into emitting unit does not change the degree of conjugation and the color of the original emitting chromophore. The relative high T_g values for the naphthalimide–carbazole dyads or triads are particularly desirable for enhancing the stability and lifetime of opto-electronic devices. Such promising bipolar emitters were successfully utilized in single-layer sandwiched EL device to avoid the layer–layer exciton quenching and micro-cavity effect. The fluorescence emission of this kind of materials can be tuned (from blue to yellow, green) with amino- and alkoxy- groups at the 4-position of naphthalimide. It implies that such naphthalimide derivatives can be custom-tuned for specific OLED applications for full color with high performance, such as good photo-stability, high fluorescent quantum yield and high electron affinity.

Acknowledgements

This work was supported by NSFC/China. Authors are indebted to Prof. A.J. Epstein and Dr. Runguang Sun (Department of Physics, the Ohio State University, USA) in the characterization of EL devices.

References

[1] K. Ziemelis, Nature 399 (1999) 4080.
[2] K.R.J. Thomas, J.T. Lin, Y.T. Tao, C.W. Ko, Chem. Mater. 14 (2002) 1354.
[3] C.H. Chen, C.W. Tang, J. Shi, K.P. Klubek, Thin Solid Films 363 (2000) 327.
[4] P.H. Liu, H. Tian, C.P. Chang, J. Photochem. Photobiol. A: Chem. 137 (2000) 99.
[5] R. Freudenmann, B. Behnisch, F. Lange, M. Hanack, Synth. Met. 111/112 (2000) 441.
[6] T. Noda, H. Ogawa, N. Noma, Y. Shirota, Adv. Mater. 9 (1997) 720.
[7] J. Kido, Phys. Wld. 12 (1999) 27.
[8] M. Berggren, O. Inganas, G. Gustafsson, J. Rasmusson, M.R. Andersson, T. Hiertbeg, O. Wennerstrom, Nature 372 (1994) 444.
[9] J. Kido, M. Kchda, K. Okuyama, K. Nagai, Appl. Phys. Lett. 61 (1992) 761.
[10] Y. Mori, in: S. Miyata, H.S. Nalwa (Eds.), Organic Electroluminescent Materials and Devices, Gordon & Breach, Amsterdam, 1997.
[11] R. Freudenmann, B. Behnisch, M. Hanack, J. Mater. Chem. 11 (2001) 1618.
[12] T. Hassheider, S.A. Benning, H.S. Kitzerow, M.F. Achard, H. Bock, Angew. Chem., Int. Ed. 40 (2001) 2060.
[13] M.R. Robinson, M.B. O'Regan, G.C. Bazan, Chem. Commun. (2000) 1645.
[14] H. Tian, T. Xu, Y.B. Zhao, K.C. Chen, J. Chem. Soc. Perkin Trans. 2 (1999) 545.
[15] K. Hasharoni, H. Levanon, S.R. Greefield, D.J. Gosztztola, W.A. Svec, M.R. Wasielewski, J. Am. Chem. Soc. 118 (1996) 10228.
[16] X. Poteau, A.I. Brown, R.G. Brown, C. Holmes, D. Matthew, Dyes Pigm. 47 (2000) 91.
[17] I. Grabchev, I. Moneva, V. Bojinov, S.J. Guittonneau, J. Mater. Chem. 10 (2000) 1291.
[18] K. Utsugi, S.J. Takano, J. Electrochem. Soc. 139 (1992) 3610.
[19] Y. Chen, R. Wehrmann, A. Elschner, Ge. Offen, 1996, DE19505942.
[20] F. Cacialli, R.H. Friend, C.M. Bouche, P. Le Barny, H. Facoetti, F. Soyer, P.J. Robin, J. Appl. Phys. 83 (1998) 2343.
[21] W.H. Zhu, M. Hu, Y.Q. Wu, H. Tian, R.G. Sun, A.J. Epstein, Synth. Met. 119 (2001) 547.
[22] C. Hu, W.H. Zhu, W.Q. Lin, H. Tian, Synth. Met. 102 (1999) 1129.
[23] X. Jiang, Y. Liu, H. Tian, X. Song, D.B. Zhu, J. Mater. Chem. 7 (1997) 1395.
[24] S.F. Zhang, D.H. Zhou, J.Z. Yang, Dyes Pigm. 27 (1995) 287.
[25] Y. Kuwabara, H. Ogawa, H. Inada, N. Noma, Y. Shirota, Adv. Mater. 6 (1994) 677.
[26] J. Bettenhausen, P. Strohriegl, W. Brü tting, H. Tokuhisa, T. Tsutsui, J. Appl. Phys. 82 (1997) 4957.

[27] K. Naito, Y. Watanabe, S. Egusa, Jpn. J. Appl. Phys. 38 (1999) 2792.
[28] C.W. Tang, S.A. VanSlyke, Appl. Phys. Lett. 70 (1997) 152.
[29] B.J. Chen, Y.Q. Liu, C.S. Lee, G. Yu, S.T. Lee, H.Y. Li, W.A. Gambling, D.B. Zhu, H. Tian, W.H. Zhu, Thin Solid Films 363 (2000) 173.
[30] J.F. Ambrose, L.L. Carpenter, R.F. Nelson, J. Electrochem. Soc.: Electrochem. Sci. Tech. 122 (1975) 876.
[31] Y. Shirota, M. Kinoshita, T. Noda, K. Okumoto, T. Ohara, J. Am. Chem. Soc. 122 (2000) 11021.